ACS OMEGA

http://pubs.acs.org/journal/acsodf

Article

Effect of Sodium Carboxymethyl Cellulose on the Dynamic Wetting Characteristics of the Dust Suppression Droplet Impacting the Coal Surface

Fangwei Han,* Yue Zhao, Mei Liu, Fuhong Hu, Yingying Peng, and Liang Ma

Cite This: *ACS Omega* 2023, 8, 18414−18424

Read Online

ACCESS | Metrics & More | Article Recommendations

ABSTRACT: The dynamic wetting behavior of droplets impacting the coal surface directly affects the efficient application of water-based dust suppression materials in coal-related industrial production. In this paper, ultrapure water, Tween-80, and sodium carboxymethyl cellulose are taken as the research objects. Using high-speed photography technology, the spreading, oscillation process, and splash morphology of many kinds of droplets during impacting the coal surface are captured. The effects of viscosity, surface tension, and impact velocity on dynamic wetting characteristics were studied. The results show that with the decrease of surface tension, the retraction and oscillation of droplets are significantly reduced. For the same kind of droplets, the greater the impact velocity, the faster the droplet spread, and the dimensionless maximum spreading coefficient (β_{max}) and dimensionless steady-state spreading coefficient (β_e) of droplets are bigger. With the increase of velocity, the time for different kinds of droplets to reach the β_{max} increases. At the same impact velocity, β_{max} and β_e of droplets (0.2% Tween-80 + 0.1% sodium carboxymethyl cellulose) are the largest, indicating that adding a small amount of sodium carboxymethyl cellulose can promote droplet spreading. With the increase of sodium carboxymethyl cellulose content, β_{max} and β_e decreased gradually. The results have a great significance to the research, development, and scientific utilization of water-soluble polymer dust inhibitors.

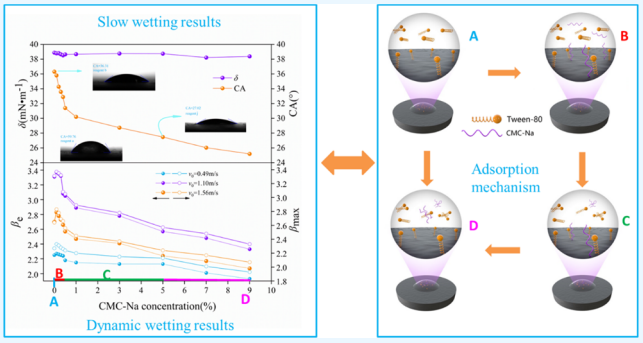

1. INTRODUCTION

The impact of droplets on the coal surface exists widely in coal mining, processing, storage, and transportation processes, such as spraying dust inhibitors, flushing roadways, and so forth.[1−3] The study of droplet impact on the coal surface not only helps to further understand the essence of the droplet impact process but is also of great significance to improve the application technology and process of water-based dust suppression materials in coal-related fields. At present, scholars mainly evaluate the wetting ability of droplets on coal by observing the static or slow wetting characteristics of droplets on the coal surface. The commonly used evaluation methods are the sessile drop method, sink test method, capillary rise method, infiltration method, and so on.[4−9] The sessile drop method is a common experimental method to measure the contact angle, which forms three-phase contact by slowly dropping droplets on the solid surface. A contact angle less than 90° means high wettability, while a contact angle greater than 90° means low wettability. Although this method is widely used, some scholars have found that the contact angle is not an effective index for evaluating surfactants.[10−13] The sink test method indirectly characterizes wettability by measuring the time required for all quantitative dust to settle into the test solution or measuring the mass fraction of dust particles that sink into water from the thin dust layer sprinkled on the surface of the solution within a certain time. The sink test experiment is affected by dust particle size distribution and powder spraying uniformity. Three to five repetitions are needed to improve accuracy.[14,15] The capillary rise test is a method to evaluate the wettability by using the capillary rise of liquid in a test tube containing dust particles.[16−18] In this method, the evaluation index is the time required for solution penetration unit height or the penetration height during unit time. The infiltration rate of the solution to the powder bed under gravity action is measured by an infiltration experiment.[19] Using the abovementioned methods to evaluate droplet wettability to coal has obvious limitations. This is because, in engineering practice, droplets have velocity.

Received: December 6, 2022
Accepted: May 4, 2023
Published: May 17, 2023

https://doi.org/10.1021/acsomega.2c07783
ACS Omega 2023, 8, 18414−18424

The time scale of slow-spreading and penetration of droplets on the coal surface is much higher than the impact contact time between droplets and coal, that is, the time before droplets retract, break, or splash from the coal surface. It can be seen that it is very critical to reveal the dynamic wetting characteristics of water-based dust suppression materials to coal.

Water-soluble polymers can improve the dust suppression ability of water-based materials. The performance of the composite system of surfactants and water-soluble polymers is significantly improved compared with the single surfactant system.[20−23] Wang et al. compared the contact angle, viscosity modulus, and foam drainage rate of different surfactants and water-soluble polymer solutions through experiments. It was found that adding water-soluble polymers significantly increased the surface viscosity of foaming agent solution, slowed down the discharge rate, and improved the stability of foam.[24] Bao et al. prepared a new type of dust suppression gel from the itaconic acid acrylic polymer and fatty alcohol polyoxyethylene ether (AEO) and bentonite by the grafting method. It was found that the dust suppressant had excellent wind erosion resistance, and the ability to wet coal dust was twice that of water. It can effectively reduce coal dust during coal transportation.[25] Zhang et al. improved the properties of guar gum (GG) with sodium sulfamate (SS) to form a modified product GGTCS and synthesized a new dust reducer with it. It was found that the dust reducer not only had excellent water saturation but also improved product's viscosity.[26] Although it has been found that the addition of water-soluble polymers to a surfactant solution will improve the dust suppression ability, the dynamic wetting characteristics of such dust suppression droplets in the impacting process have not been revealed.

It is very important to observe and understand the dynamic wetting characteristics of droplets impacting the coal surface. The existing research shows that the main factors affecting the droplet dynamic wetting behavior include impact velocity, impact angle, droplet size, physical and chemical properties of the droplet (viscosity, surface tension, etc.), surface wettability and solid surface roughness, and so forth.[27−30] For example, Han et al. studied the dynamic wetting behavior of underwater oil droplets impacting the smooth brass substrate and 316L stainless steel using a high-speed camera technology. It was found that with the increase of dimensionless time, the dimensionless spread length of the droplet had a negative correlation with the contact angle.[31] Lunkad et al. used the VOF method to numerically simulate the collision and spread of droplets on horizontal and inclined surfaces and studied the effects of surface inclination, surface wettability, liquid properties, and impact velocity on droplet impact dynamics. The results showed that when the static contact angle was less than 90°, the droplet would spread and deposit on the solid surface.[32] Liu et al. used the CLSVOF method to study the effect of surface wettability on the droplets impact on the spherical surface. It was found that when the impact velocity was constant, the maximum expansion factor and the time required to reach the maximum expansion factor decreased with the increase of contact angle.[33,34] Banks et al. studied the process of spray droplets impacting the solid surface and found that the kinematic viscosity, impact velocity, and surface tension effect of droplets played an important role in the oscillation. High viscosity droplets often stopped oscillation faster than low viscosity droplets.[35] Nefzaoui and Skurtys used the high-speed camera technology to study the dynamic wetting behavior of different kinds of droplets after impacting the glass ball and found that the spread, retreat, and absorption of droplets were affected by fluid viscosity and surface tension, especially when the kinetic energy was high.[36] To sum up, it can be found that most of the existing studies are about the process of water droplets, glycerol, and other liquid droplets impacting the solid plane, while there are few experimental studies about the process of droplets impacting the coal surface, especially the droplets containing surfactants and water-soluble polymers.

In this article, the influence of sodium carboxymethyl cellulose on the dynamic wetting behavior of Tween-80 droplets impacting the coal surface is studied using high-speed camera technology. The effects of droplet physical properties, impact velocities, and water-soluble polymer addition on droplet dynamic wetting behavior are analyzed. It not only solves the limitation of the existing slow-wetting evaluation methods but also fills the blank of the research on the dynamic wetting behavior of the coal surface impacted by droplets containing surfactants and water-soluble polymers. The results have a great significance to the research, development, and scientific utilization of water-soluble polymer dust inhibitors.

2. METHODS AND MATERIALS

2.1. Experimental System. As shown in Figure 1, the experimental system mainly includes the droplet generator (composed of a peristaltic pump, a luer connector, a dispensing flat needle, etc.), a sample loading platform, supports, a high-speed camera, and so forth. Different kinds of droplets are produced by the droplet generator. The droplet diameter is determined by the diameter of the flat needle. Droplets drop freely under the action of gravity. Different impact velocities are obtained by adjusting the initial falling height of droplets.

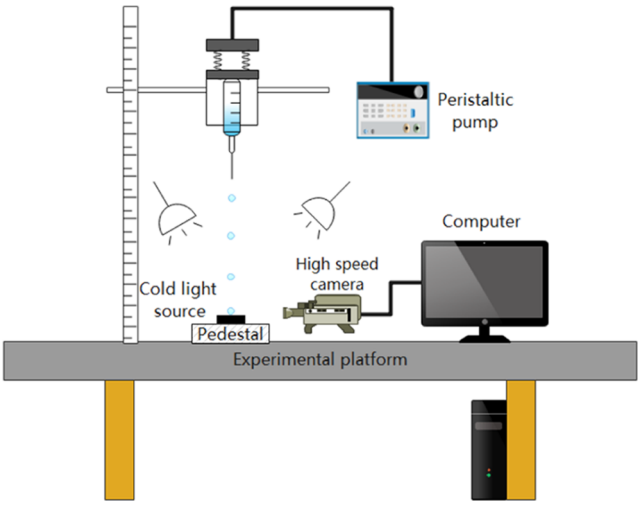

Figure 1. Experimental system diagram.

A high-speed digital camera (Vision Research Inc.; Phantom VEO340S) is used to get time-series images of the interaction between droplets and the coal surface. The camera lens adopts a high-precision macro optical lens (Nicon; AF-S micro Nikkor 105 mm). Continuous light (XD-303) illuminates the observation area, which enables one to get clear images even at a short exposure time. The interaction process is recorded by the high-speed camera at 1500 fps. The resolution of images is 1920 × 1080 pixels. The collected images are transmitted to the computer through the data acquisition card and displayed on the computer in real time through the software analysis system. All

https://doi.org/10.1021/acsomega.2c07783
ACS Omega 2023, 8, 18414−18424

Table 1. Physical Parameters of Different Reagents

serial number	solution type	temperature T (°C)	density ρ (kg/m^3)	viscosity η (mPa·s)	droplet diameter d_0(mm)
reagent a	ultrapure water	25	998	0.89	2.61
reagent b	0.2% Tween-80	25	998	1.02	2.26
reagent c	0.2% Tween-80 + 0.1% CMC-Na	25	998	1.13	2.25
reagent d	0.2% Tween-80 + 0.2% CMC-Na	25	998	1.18	2.19
reagent e	0.2% Tween-80 + 0.3% CMC-Na	25	998	1.35	2.22
reagent f	0.2% Tween-80 + 0.4% CMC-Na	25	998	1.44	2.20
reagent g	0.2% Tween-80 + 0.5% CMC-Na	25	998	1.63	2.23
reagent h	0.2% Tween-80 + 1% CMC-Na	25	998	3.35	2.25
reagent i	0.2% Tween-80 + 3% CMC-Na	25	999	9.32	2.25
reagent j	0.2% Tween-80 + 5% CMC-Na	25	999	19.70	2.29
reagent k	0.2% Tween-80 + 7% CMC-Na	25	1000	85.0	2.29
reagent l	0.2% Tween-80 + 9% CMC-Na	25	1002	117.0	2.28

experiments were conducted three times with the temperature of 25 °C and humidity range of 51.0−55.0%, respectively.

2.2. Preparation of Solutions. Table 1 shows the physical property parameters of various reagents used in the experiment. Reagent a is ultrapure water. Reagent b is a 0.2% Tween-80 solution. The other ten kinds of Tween-80 mixed solutions contain sodium carboxymethyl cellulose (CMC-Na), namely, reagent c ∼ reagent l. The preparation method of reagent c ∼ reagent l is to take a certain amount of prepared reagent b solution and add sodium carboxymethyl cellulose solution with mass fractions of 0.1, 0.2, 0.3, 0.4, 0.5, 1, 3, 5, 7, and 9%, respectively. The water used for preparing the experiment solution is ultrapure water. Tween-80 and CMC-Na were purchased from Shandong Yousuo Chemical Technology Co., Ltd. The viscosity of different kinds of droplets was measured by a rotating viscometer (Shanghai Pingxuan Scientific Instrument Co., Ltd., NDJ-5S).

2.3. Preparation of Coal Samples. The coal sample used in the experiment was bituminous coal, collected from the Xindingtai coal mine, Jinzhong City, Shanxi Province, China. After the raw coal was obtained, the surface dust and other impurities were washed with ultrapure water, sealed, dried, and then screened to 80−100 meshes by a screening machine (Lishui Boke Hardware Co., Ltd.; ZF-J-11). Before each tableting, we weigh coal samples of the same quality with an electronic balance. Then, a tablet press was used to obtain coal tablets with a diameter of 20 mm and a thickness of 3 mm under a working pressure of 25 MPa.

2.4. Contact Angle Measurement. During the measurement, the volume of the solution injector was 50 μL, and the accuracy was 0.2 μL. Adjusting the illumination brightness to make the overlap between the horizontal line of the measuring interface and the coal surface clear. The drop contact angle was measured manually by hypsometry. To ensure the accuracy of the experimental data, each droplet was measured three times continuously with a contact angle measuring instrument (Shanghai Zhongchen Digital Technology Equipment Co., Ltd., JC2000D1) to obtain the average value.

2.5. Surface Tension Measurement. The surface tension was measured by the platinum plate method on a surface tensiometer (Shanghai Zhongchen Digital Technology Equipment Co., Ltd., JK99D). Each solution was measured three times to obtain the average surface tension value, and the difference between the three test results was within 0.2 mN/m. Before each measurement, the platinum tablet was washed with distilled water and dried on an alcohol lamp.

2.6. Molecular Dynamics Simulation. Based on the chemical structures and properties of bituminous coal, Tween-80, CMC-Na, and ultrapure water, molecular models were established using Materials Studio software. Using the Amorphous Cell tools module to establish each component box and geometric optimization. Figure 2 shows the models.

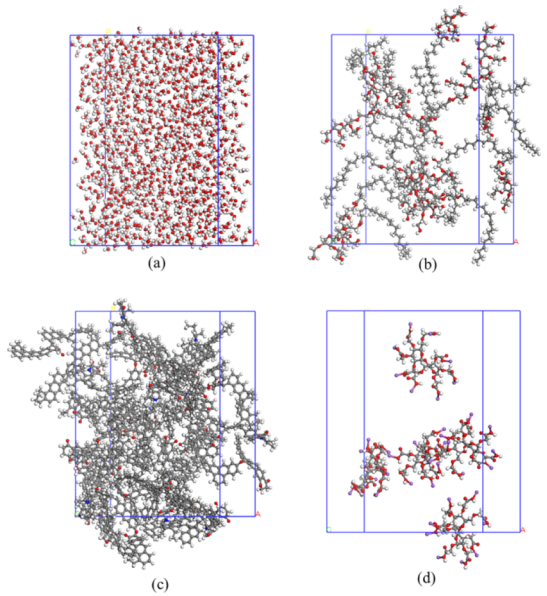

Figure 2. AC models, in which (a−d) are ultrapure water, Tween-80, bituminous coal, and CMC-Na, respectively.

After the optimization, bituminous coal, Tween-80, water, and CMC-Na were added to the rectangular simulation unit with the size of 50 Å × 50 Å × 200 Å, and then, the vacuum layer was established according to the periodic boundary conditions. Using dynamics tasks in the Forcite module, the quality was set to fine. According to the chemical properties and application range of various force fields, the COMPASS II force field was adopted. To select initial conditions similar to the experimental environment, an NVT ensemble was used in the simulation. The temperature was controlled at 298 K. The time step was set to 1.0 fs, and the total time was set to 400 ps. For simulation purposes, Van Der Waals interaction with a cutoff radius of 12.5 Å was used, and the accuracy was set to 0.001 kcal/mol. In the process of molecular dynamics simulation, coal molecules were fixed. This can more intuitively display the dynamic behavior of surfactant molecules and CMC-Na molecules, thus shortening

https://doi.org/10.1021/acsomega.2c07783
ACS Omega 2023, 8, 18414−18424

the simulation time. At the same time, in the authentic experimental process, the actual distribution of coal molecules is fixed. Other studies also show that these constraints have little effect on calculation results.[37]

2.7. Characterization Parameters of Dynamic Wetting Characteristics. After the droplet impacts the coal surface, under the combined action of surface tension, inertial force, and other forces, the droplet spreads along the coal surface, and the contact area of the droplet on the coal surface increases gradually. When the spreading area reaches maximum, the liquid continues to diffuse, making the edge thicker and forming eddy currents at the edge, and the spreading velocity decreases to 0 m/s after a few milliseconds. The kinetic energy is completely transformed into deformation energy, viscous dissipation, and so forth. Then, the droplet begins to contract from outside to inside under the action of surface tension. When the droplet spreading radius shrinks to the minimum value, the contraction velocity decreases to 0 m/s again, and then, the droplet spreads outward again, that is, oscillation occurs. When the oscillation is over, the droplets standstill on the coal surface. It can be seen that the free surface position (solid-liquid-gas contact surface) changes with time during the spreading process. The spreading diameter of the droplet on the coal surface is an important parameter for analyzing the impact characteristics, as shown in Figure 3.

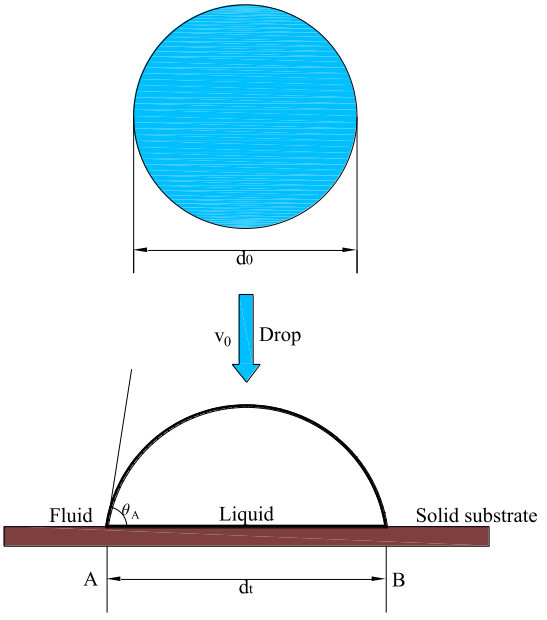

Figure 3. Transient diagram of droplet spreading on the coal surface.

The initial droplet diameter (d_0) is used to dimensionless the spreading diameter. The dimensionless spreading coefficient is obtained β

$$\beta = \frac{d_t}{d_0} \tag{1}$$

where d_t is the spreading diameter of the droplet impacting the coal surface.

To describe the droplets spreading after impact, the dimensionless maximum spreading coefficient (β_{max}) and dimensionless steady-state spreading coefficient (β_e) are taken as important research objects, which are defined as follows

$$\beta_{max} = \frac{d_{max}}{d_0} \tag{2}$$

$$\beta_e = \frac{d_e}{d_0} \tag{3}$$

where d_{max} is the maximum spreading diameter of the droplet after impact, and d_e is the final steady spreading diameter of the droplet.

Dimensionless time is defined as follows

$$\tau = \frac{tv_0}{d_0} \tag{4}$$

where t is the different time when the droplet impacts the coal surface, and v_0 is the impact velocity.

According to the collected image information, the impact velocity v_0, the initial droplet diameter d_0, and the maximum spreading diameter d_{max} are measured. The influence of the water-soluble polymer on the dynamic characteristics of Tween-80 droplets impacting the coal surface is understood through dimensionless spreading coefficient, Reynolds number (Re), and Weber number (We).

$$Re = \frac{\rho v_0 d_0}{\mu} \tag{5}$$

$$We = \frac{\rho v_0^2 d_0}{\delta} \tag{6}$$

where ρ is the droplet density, μ is the dynamic viscosity coefficient of the droplet, and δ is the surface tension coefficient of the droplet.

3. RESULTS AND DISCUSSION

3.1. Effect of Physical Properties on Dynamic Wetting Behaviors of Droplets. Continuous images of droplets impacting the coal surface are obtained from the experimental data. Figure 4a–c respectively show the process of reagent a (ultrapure water), reagent b (0.2% Tween-80), and reagent j (0.2% Tween-80 + 5% CMC-Na) droplets impacting the coal surface with the same initial velocity v_0 = 0.49 m/s. The droplet impact process can be divided into three stages: spreading, oscillation, and equilibrium. At the initial stage of the impact, the contact between the droplet and the wall is very small, and the upper surface of droplets remains approximately spherical. With the increase of time, droplets begin to spread, and the spreading velocity of different droplets shows significant differences. The time required for reagent b droplets containing the surfactant to reach the maximum spreading coefficient is 4.69 ms, and so the average spreading velocity is 1.06 m/s, which is the fastest among the three reagents. The time required for ultrapure water droplets to reach the maximum spreading coefficient is 6.03 ms, and so the average spreading velocity is 0.94 m/s, which is the slowest among the three reagents. The abovementioned results show that the addition of surfactants will promote the spreading of droplets. This is because the direction of surface tension is always perpendicular to the liquid surface. When the droplet spreading area increases, the area affected by surface tension also increases. In the horizontal direction, the action direction of surface tension is opposite to the spreading direction, which is one of the resistances of spreading. When the surfactant is added, the surface tension decreases, and the droplet spreading resistance decreases significantly.

https://doi.org/10.1021/acsomega.2c07783
ACS Omega 2023, 8, 18414−18424

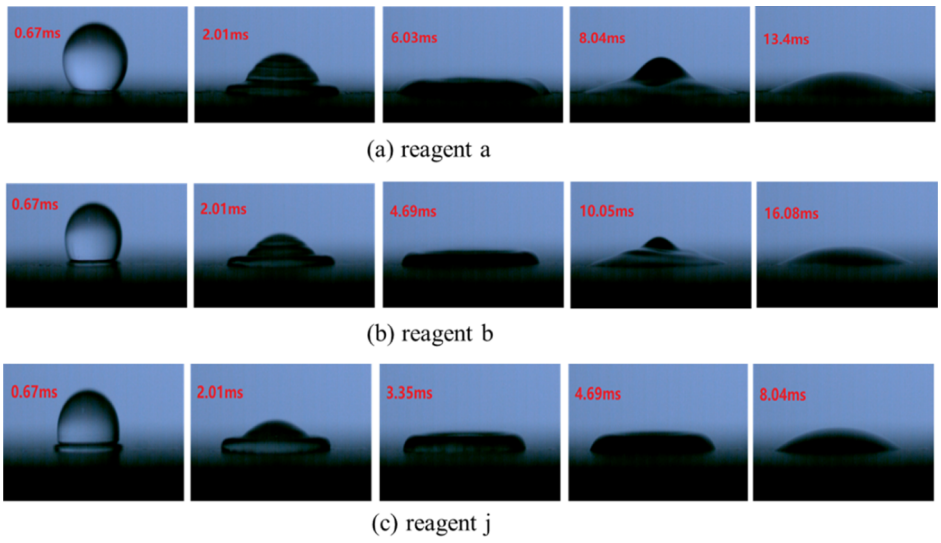

Figure 4. Dynamic process of droplets impacting the coal surface at v_0 = 0.49 m/s.

After reaching the maximum spreading diameter, the droplet of ultrapure water begins to retract and then continues to oscillate until it reaches equilibrium. At equilibrium, the droplet is a spherical crown. Its β_e is 2.20, less than its β_{max} 2.25, indicating that the ultrapure water droplets retract after impacting. When the droplet spreads to the maximum diameter, the surface tension is one of the driving forces of droplet retraction. The droplets with high surface tension and low viscosity will obviously retract under the action of surface tension after spreading to a certain extent and reach equilibrium after multiple oscillations. The surface tension of ultrapure water is much greater than that of the other two reagents, that is, the coalescence energy of ultrapure water droplets is much greater than them, so its retraction phenomenon is the most obvious. The droplet of reagent b retracts slightly, and its β_e 2.25 is slightly less than the β_{max} 2.27. However, reagent j has no retraction phenomenon, β_e and β_{max} are the same, both of which are 2.13. The edge of reagent j is relatively smooth and gentle in the process of contacting the coal surface. Comparing the droplet spreading process of reagent b and reagent j, it can be found that the droplet composition plays an important role in the droplet spreading process. As shown in Figure 5a, when

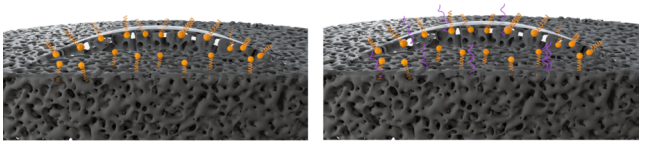

Figure 5. Pinning effect of droplets on the coal surface.

reagent b spreads along the coal surface, the molecules at the lower part of the droplets spread at first on the coal surface under the action of kinetic energy, and the spreading diameter increases accordingly. When the droplet reaches the maximum spreading diameter, a small number of molecules in the lower part of the droplet have a pinning effect on the coal surface, but then the droplet still retracts. This is because although the hydrophobic carbon chain in the Tween-80 molecule will interact with the hydrophobic groups on the coal surface, this interaction does not effectively prevent the retraction of droplets. As shown in Figure 5b, water-soluble polymer CMC-Na is added to the reagent j droplet. In addition to the interaction between the Tween-80 molecule and the coal surface, CMC-Na has a large molecular weight, contains many hydrophilic hydroxyl and ether bonds, and also interacts with hydrophilic groups on the coal surface. Therefore, components of reagent j droplets have stronger interaction with coal molecules and a stronger pinning effect. Compared with reagent b, the retraction phenomenon is significantly inhibited.

The surfactant can effectively reduce the surface tension and improve the wetting effect. As shown in Figure 6, according to

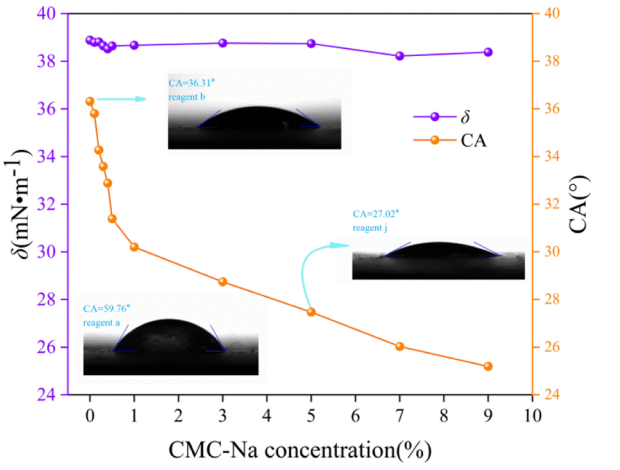

Figure 6. Combination diagram of surface tension and contact angle of different droplets.

the surface tension test results, the surface tension of reagent a is 71.97 mN/m. The surface tensions of reagent b and reagent j are 38.88 and 38.97 mN/m, respectively. The surface tension values of the two reagents are very close and significantly less than reagent a. It can be seen that the addition of Tween-80 can significantly reduce the surface tension of water, while the addition of CMC-Na has little effect on the surface tension. Surface tension is often used to evaluate the wettability of liquid on a solid surface. Generally, the larger the surface tension, the harder the solution is to wet the solid surface. The spontaneous diffusion of liquid on the coal surface requires a surface tension

https://doi.org/10.1021/acsomega.2c07783
ACS Omega 2023, 8, 18414−18424

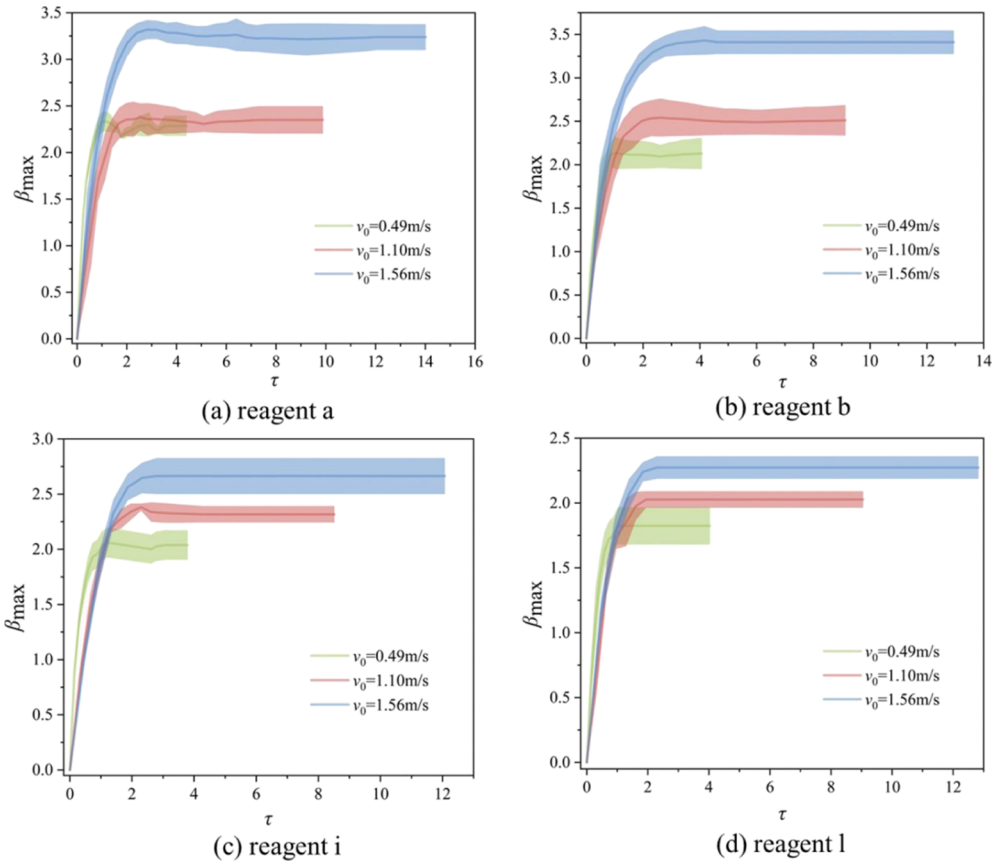

Figure 7. Variation diagram of β_{max} of reagent a, b, i, l at different velocities.

of less than 45 mN/m (critical surface tension).[38] The surface tension of reagent j is lower than the critical surface tension and significantly lower than that of reagent a. If the surface tension is used to evaluate, reagent j should be easier to wet the coal surface. However, according to the impact experiment, the β_{max} of reagent j is less than that of reagent a, and the wetting ability is obviously lower than reagent a. The result shows that surface tension has obvious limitations in evaluating the wettability of solutions, and it cannot effectively evaluate the wettability of droplets in the process of dynamic impacting. After the surface tension reaches the critical value, the surface tension is no longer the dominant factor. Other factors, such as the addition of water-soluble polymers, begin to affect the wettability of droplets.

The results show that the contact angle of droplets is gradually reduced after adding CMC-Na. The contact angle is often used to evaluate the wettability of liquid on a solid surface. Generally, the smaller the contact angle, the better the wettability is. The contact angle of reagent j is smaller than that of reagent a. If evaluated according to the contact angle, reagent j should be easier to wet the coal surface. However, from the impact experiment, the β_{max} of reagent j is less than that of reagent a, and the wetting ability is obviously lower than reagent a. It can be seen that the contact angle also has obvious limitations in evaluating the wettability of solutions, and it cannot effectively evaluate the wettability of droplets in the process of dynamic impacting. The contact angle is the angle formed by the tangent line between the solid−liquid interface and the gas−liquid interface. The contact angle measured by the sessile drop method can only be regarded as the apparent contact angle, not the actual contact angle, and can only be used as a qualitative method.[39] This is because the contact angle is also affected by other factors such as the adsorption of molecules on the solid surface and the intermolecular force inside the droplet. The surface tension of reagent b and reagent j is close, but the contact angle is significantly different. This may be because the water-soluble polymer CMC-Na does not tend to exist on the liquid surface and change the droplet surface tension. However, when reagent j drops on the coal surface, there is a stronger van der Waals force between CMC-Na and oxygen-containing groups on the coal surface, which promotes the spread of droplets on the coal surface and reduces the contact angle.

3.2. Effect of Impact Velocity on Dynamic Wetting Behaviors of Droplets. The impact velocity has basically the same trend for the dynamic wetting of the coal surface by different droplets. Figure 7 only shows a variation diagram of four different droplets β_{max} at different velocities. The impact velocities are 0.49, 1.10, and 1.56 m/s, respectively. (Corresponding *We* is about 13, 70, and 141).

For the same droplet, the higher the impact velocity is, the faster the spreading velocity is, and the larger the β_{max} is. This is because the impact velocity directly determines the impact kinetic energy. Obviously, the higher the velocity, the larger the impact energy. For reagent a droplets, after reaching the β_{max}, there is obvious retraction due to the large surface tension. Reagent b droplets spread very violently and rapidly in the early stage and then slightly retracted. By observing the experimental process, it is found that reagent a droplets will show the morphological characteristics of splashing movement when they impact the coal surface at a high velocity, as shown in Figure 8. The reagent b droplets do not splash, indicating that the velocity also plays an important role in the splash process. Under the

https://doi.org/10.1021/acsomega.2c07783
ACS Omega 2023, 8, 18414−18424

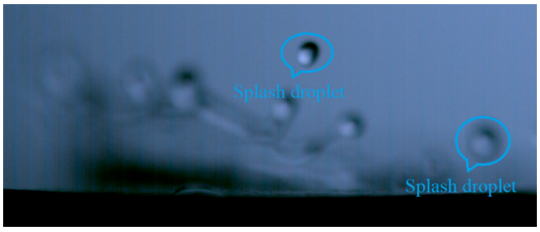

Figure 8. Splash diagram of reagent a.

experimental conditions in this paper, the critical velocity v_c of the reagent a droplet splashing on the coal surface is 2.48 m/s.

In addition, we calculated the relationship between *We* and β_{max} and observed whether there was an obvious functional relationship between them. As shown in Figure 9, the results

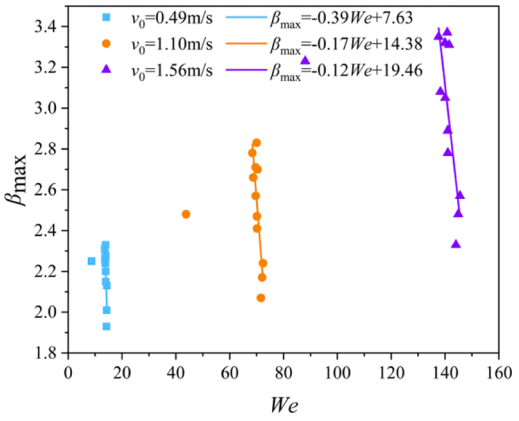

Figure 9. Fitting diagram of *We* and β_{max} of reagent b ∼ reagent l at different velocities.

show that under the conditions in this paper, when the *We* is almost the same, β_{max} values can vary greatly. There is a linear relationship between them through data fitting, which does not include the data of water droplets. It is also found that the slope of the fitting curve is very small, indicating that the prediction value using *We* is not accurate at this time. So, it is necessary to further discuss the influence of other parameters, such as *Re* and so on.

Table 2 lists the β_{max} and τ when twelve kinds of droplets impact the coal surface. The results show that the β_{max} and the τ growth with the increase of the impact velocity. This is because

Table 2. β_{max} and τ of Different Droplets

	0.49 m/s		1.10 m/s		1.56 m/s	
solution type	β_{max}	τ	β_{max}	τ	β_{max}	τ
reagent a	2.25	1.13	2.48	2.26	3.23	2.8
reagent b	2.27	1.02	2.70	2.61	3.31	2.86
reagent c	2.33	1.17	2.83	2.29	3.37	2.79
reagent d	2.31	1.2	2.78	2.36	3.35	2.86
reagent e	2.28	1.18	2.71	2.32	3.32	2.82
reagent f	2.26	1.19	2.66	2.35	3.08	2.85
reagent g	2.24	1.18	2.57	2.31	3.05	2.81
reagent h	2.20	1.17	2.47	2.29	2.89	2.79
reagent i	2.15	1.17	2.41	2.29	2.78	2.79
reagent j	2.13	1.0	2.24	1.93	2.57	2.28
reagent k	2.01	1.0	2.17	1.93	2.48	2.28
reagent l	1.93	1.01	2.07	1.94	2.33	2.29

no matter which kind the droplet is, the larger the impact velocity, the greater the diffusion degree is, resulting in the total diffusion time longer.

3.3. Effect of CMC-Na Additional Amount on Dynamic Wetting Behaviors of Droplets. To study the effect of CMC-Na additional amount on the dynamic wetting behaviors of droplets, the dynamic wetting behaviors of reagent c ∼ reagent l are compared experimentally. The experiment results are shown in Figure 10. The β_{max} and β_e of the mixed solution all increased

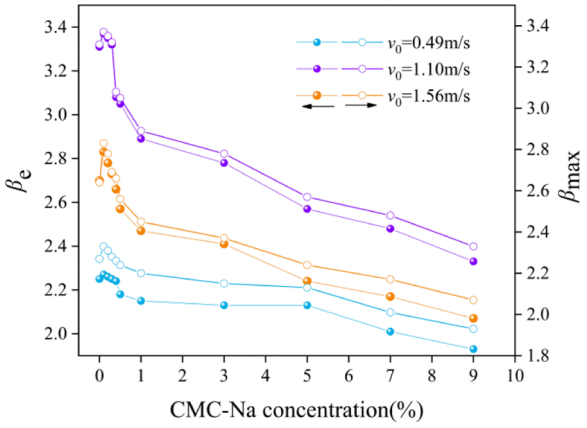

Figure 10. Variation diagram of droplets β_{max} and β_e with CMC-Na additional amount.

initially and then decreased. When the additional concentration of CMC-Na is 0.1%, the β_{max} and β_e are the maximum. According to the abovementioned experimental results, it is easy to know that the surface tension of mixed droplets is basically unchanged with the increase of CMC-Na content. Obviously, the promotion of the droplet spreading by 0.1% CMC-Na is not achieved by changing the surface tension. It may be that the addition of CMC-Na strengthens the interaction between droplets and the coal surface. As shown in Figure 11a, when CMC-Na is not added, Tween-80 molecules form an unsaturated adsorption layer at the interface, and there is no micelle inside the droplet. When adding low concentration CMC-Na, as shown in Figure 11b, the CMC-Na molecule interacts with the hydrophilic group in the coal molecule. Currently, there is almost no micelle structure in the mixed solution. The droplet density and initial kinetic energy increase, but the slight addition of CMC-Na has not significantly changed the droplet viscosity, which is not enough to offset the kinetic energy increment. It can be observed that adding a small amount of water-soluble polymers to the surfactant solution will promote its spreading on the coal surface. With the increase of CMC-Na concentration, as shown in Figure 11c, CMC-Na molecules tend to form their own micelle structure, which increases the viscosity of droplets. When the additional amount of CMC-Na further increases, as shown in Figure 11d, the CMC-Na single-molecule no longer exists. In addition to self-winding to form micelles in the mixed solution, its molecules will also wind with Tween-80 molecules, which greatly increase the viscosity of droplets and hinder the spreading of droplets.

Figure 12 shows the change of β_{max} of 10 different mixed droplets with time when v_0 = 0.49 m/s ($We \approx 13$). The abovementioned experiments show that with the further increase of CMC-Na addition, the viscosity increases gradually. The β_{max} of droplets decreases with the increase of the additional amount. Compared with low viscosity droplets, the spreading

https://doi.org/10.1021/acsomega.2c07783
ACS Omega 2023, 8, 18414−18424

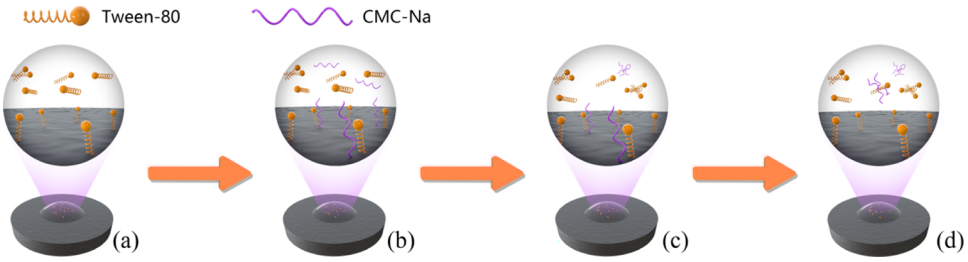

Figure 11. Coal surface adsorption under different CMC-Na additional amount, in which (a−d) represent the addition amount of CMC-Na in the solution as 0, 0.1−0.3, 0.4−5, and 7−9%, respectively.

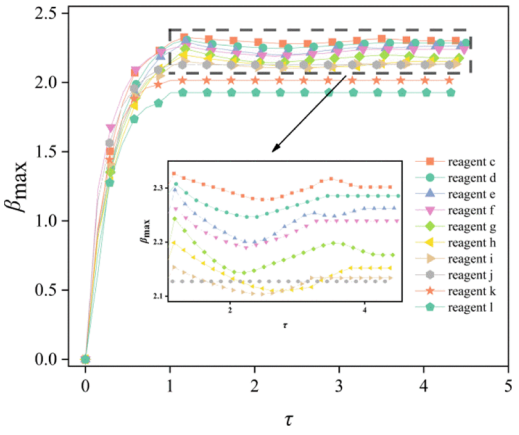

Figure 12. Variation diagram of reagent c ∼ reagent l β_{max} at v_0 = 0.49 m/s.

velocity of high viscosity droplets is slower, indicating that viscosity plays an inhibitory role in spreading. In addition, after adding high concentration CMC-Na, there is no obvious retraction oscillation phenomenon of droplets, and the β_{max} of droplets is almost equal to the final β_e. This is owing to the direction of viscous force is opposite to the droplet velocity. When the droplet viscosity increases obviously, the amplitude of droplet reduces, and retraction decreases gradually under the action of viscous dissipation. The larger the viscosity of the droplet, the greater the viscous dissipation caused by the shear stress in the solid−liquid contact area and the less the residual energy in the later stage of droplet spreading, which makes it difficult for the droplet to retract and oscillate. In addition, the splash phenomenon of mixed droplets is also suppressed. The β_{max} of droplets with larger viscosity is smaller, and the spreading is slower.

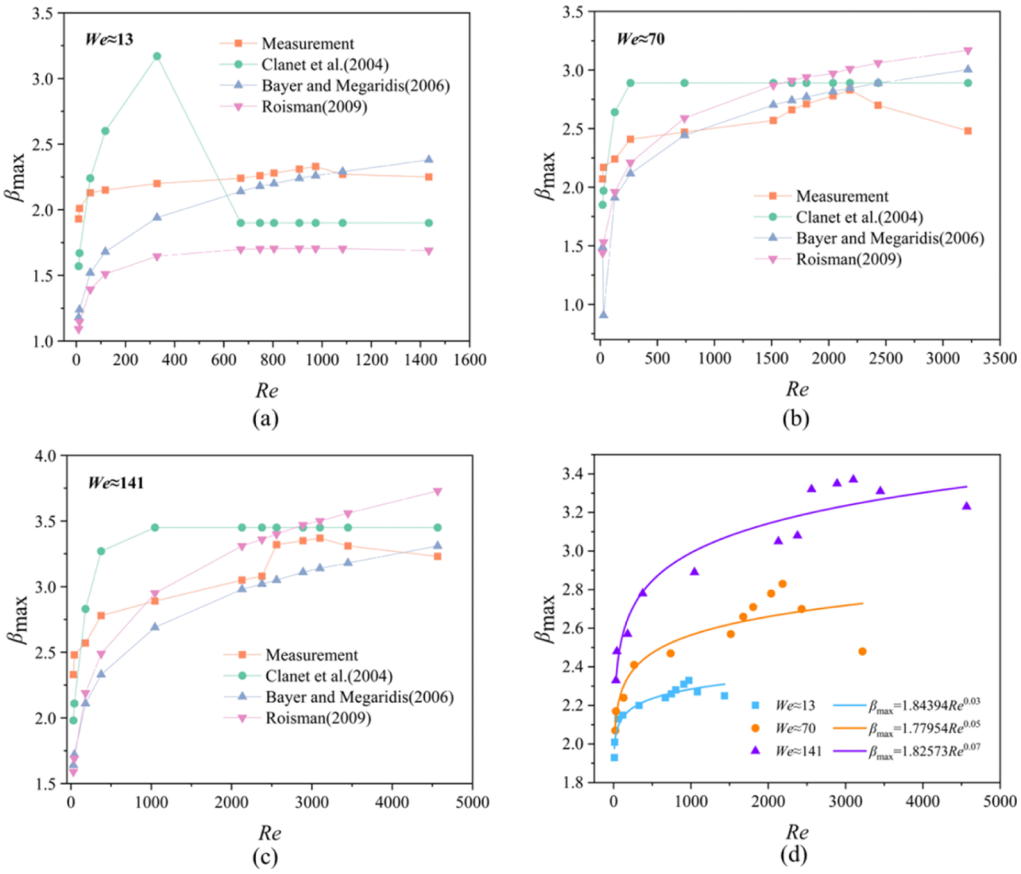

Figure 13. Comparison between experimental data and different prediction models data on the relationship between *Re* and β_{max}; (a−c) *We* of 13, 70, and 141 and (d) fitting curve between *Re* and β_{max}.

https://doi.org/10.1021/acsomega.2c07783
ACS Omega 2023, 8, 18414−18424

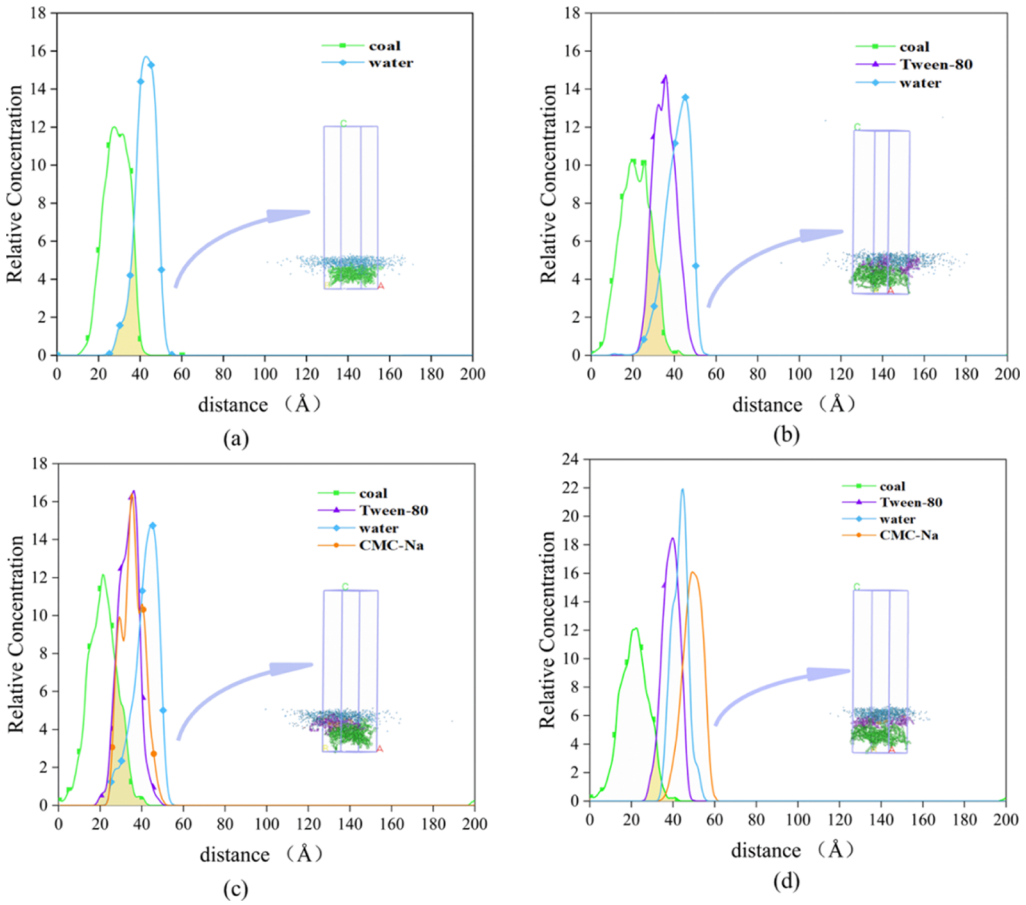

Figure 14. Adsorption density of bituminous coal, water, Tween-80, and CMC-Na along *Z* axis; (a,b) water/bituminous coal and water/Tween-80/bituminous coal systems and (c,d) water/Tween-80/CMC-Na/bituminous coal systems with 2 and 5 CMC-Na.

The abovementioned results show that viscosity plays a dual role in the spreading of mixed droplets on the coal surface. So this paper studies the relationship between *Re* and β_{max}. As shown in Figure 13a, under the lower *We*, with the increase of *Re*, β_{max} first increases and then decreases, showing nonmonotonicity. This is consistent with the result curve trend of Qin et al.[40] However, the β_{max} value differ greatly. As shown in Figure 13b,c, when $We \approx 70$ and $We \approx 141$, this non-monotonic trend is more similar to the research results of Clanet et al., and the difference in β_{max} value between the two is very small. It is also close to the predicted β_{max} value of Bayer and Roisman et al.[41−43] Due to the double effect of viscosity, the previous prediction formula is highly consistent with the experimental data at a high *We*. However, the error between the experimental data at low *We* and the previous formula is large. Most of the previous studies are glycerol, ethanol, alkanes, pure water droplets, and so forth, while this paper studied the mixed droplets of Tween-80, CMC-Na, and ultrapure water solution. In this paper, the surface tension fluctuated little when the concentration of solution changed, and there might be interaction between water-soluble polymers, which affected the experimental results. Second, the impact on the smooth stainless-steel surface and the impact on the coal surface will also cause differences. It can be found that the previous experimental conclusions of droplets impact on the solid surface are not completely applicable to the case of droplets impact on coal surface. Therefore, this paper studies the relationship between β_{max} and *Re*. When $13 < We < 141$, as shown in Figure 13d, through fitting, there is a power exponential relationship between the two. However, this relationship is only applicable to the process of droplet impacting the coal surface under this condition.

To further analyze the effect of CMC-Na addition of Tween-80 containing droplets wetting on the coal surface, the relative concentration distribution of each component in water/bituminous coal, water/Tween-80/bituminous coal, and water/Tween-80/CMC-Na/bituminous coal system along the surface perpendicular to bituminous coal is analyzed by using Forcite module. Figure 14a shows the concentration distribution curve of water molecules on the surface of bituminous coal, in which the peak value represents the concentrated distribution area of molecules. Bituminous coal molecules are mainly distributed in the range of 10−40 Å, water molecules are distributed in the range of 25−55 Å, and some water molecules overlap with bituminous coal molecules. Figure 14b shows that bituminous coal molecules are mainly distributed in the range of 10−40 Å, Tween-80 molecules are mainly distributed in the range of 20−50 Å, and water molecules are distributed in the range of 20−55 Å. At this time, Tween-80 and water molecules have a large overlapping range with bituminous coal molecules, indicating that Tween-80 molecules promote the adsorption and wetting behavior of bituminous coal to water molecules. As shown in Figure 14c, after adding a small amount of CMC-Na, the main distribution range of Tween-80 molecules is expanded to 15−50 Å, the distribution range of water molecules is 20−55 Å, and the CMC-Na molecules are mainly distributed in 22−50 Å. At this time, the overlapping range of water molecules and bituminous coal molecules is basically unchanged, and there are a large number of overlapping ranges of Tween-80 molecules,

https://doi.org/10.1021/acsomega.2c07783
ACS Omega 2023, 8, 18414−18424

CMC-Na molecules, and bituminous coal molecules, which further enhances the wettability of the system. As shown in Figure 14d, when the amount of CMC-Na is further added, the overlapping areas of the Tween-80 molecule, water molecule, CMC-Na molecule, and bituminous coal molecule are greatly reduced, and the wettability of the system is reduced. The abovementioned simulation results are basically consistent with the experimental results, which shows the reliability and accuracy of the experimental results.

4. CONCLUSIONS

In this paper, a study on the dynamic wetting process of water-soluble polymer regulating Tween-80 droplets impacting the coal surface is carried out. The main conclusions are as follows:

(1) When the velocity is low, ultrapure water droplets produce obvious retraction oscillation under the action of surface tension and reach equilibrium after a considerable oscillation period. The retraction phenomenon of surfactant droplets and mixed droplets added with CMC-Na is small, or even does not occur. It shows that the addition of surfactant will promote the spread of droplets. There is the pinning effect in the process of the droplet spreading, and the pinning effect is strengthened after adding CMC-Na.

(2) In the dynamic wetting process of droplets impacting the coal surface, there are some limitations in taking the solution surface tension and contact angle as the evaluation index. The dimensionless maximum spreading coefficient (β_{max}) and dimensionless steady-state spreading coefficient (β_e) can better evaluate the dynamic wetting characteristics of droplets.

(3) With the increase of impact velocity, the β_{max} of different droplets increases, and the time to reach the β_{max} extended. For the same droplet, the β_{max} and the impact velocity show a positive correlation. The droplets with large velocities can reach a larger diffusion range. When the β_{max} of droplets increases with the increase of velocity, the β_e also increases. The critical velocity of ultrapure water droplets splashing on the coal surface is 2.48 m/s.

(4) After adding CMC-Na, the β_{max} of the mixed solution increases first and then decreases with the increase of the amount of CMC-Na. When the concentration of CMC-Na was 0.1%, the promotion effect was the most significant. Molecular dynamics simulation results show that the wettability of the water/Tween-80/bituminous coal system is better than the water/bituminous coal system. On this basis, the wettability of the water/Tween-80/CMC-Na/bituminous coal system with a small amount of CMC-Na is further enhanced.

AUTHOR INFORMATION

Corresponding Author

Fangwei Han − *College of Safety Science and Engineering, Liaoning Technical University, Huludao 125105 Liaoning Province, China; Key Laboratory of Mine Thermodynamic Disasters and Control, Ministry of Education, Liaoning Technical University, Huludao 125105 Liaoning Province, China;* orcid.org/0000-0002-7605-8917; Phone: +86 13700196395; Email: hanfangwei@lntu.edu.cn; Fax: +86 13700196395

Authors

Yue Zhao − *College of Safety Science and Engineering, Liaoning Technical University, Huludao 125105 Liaoning Province, China*

Mei Liu − *College of Safety Science and Engineering, Liaoning Technical University, Huludao 125105 Liaoning Province, China*

Fuhong Hu − *College of Safety Science and Engineering, Liaoning Technical University, Huludao 125105 Liaoning Province, China*

Yingying Peng − *College of Safety Science and Engineering, Liaoning Technical University, Huludao 125105 Liaoning Province, China*

Liang Ma − *College of Safety Science and Engineering, Liaoning Technical University, Huludao 125105 Liaoning Province, China*

Complete contact information is available at: https://pubs.acs.org/10.1021/acsomega.2c07783

Author Contributions

F.H.: Conceptualization, resources, methodology, writing—original draft, project administration, funding acquisition, and supervision. Y.Z.: Writing—original draft, writing—review and editing, data curation, and methodology. M.L.: Formal analysis, validation, data curation, and writing—review and editing. F.H.: Conceptualization, writing—original draft, and investigation. Y.P.: Conceptualization, data curation, and methodology. L.M.: Writing—original draft and data curation.

Notes

The authors declare no competing financial interest.
All data generated or analyzed during this study are included in this paper.

ACKNOWLEDGMENTS

This work was supported by the Natural Science Foundation of Liaoning Province [grant number 2022-MS-396] and National Natural Science Foundation of China [grant number 52074192]. The authors deeply appreciate the support from the staff of Key Laboratory of Mine Thermodynamic Disasters and Control. We are also grateful to the editors for their key work.

REFERENCES

(1) Wang, P. F.; Tan, X. H.; Cheng, W. M.; Guo, G.; Liu, R. H. Dust removal efficiency of high pressure atomization in underground coal mine. *Int. J. Min. Sci. Technol.* **2018**, *28*, 685−690.

(2) Cheng, W. M.; Wang, H.; Sun, B.; Ma, Y. Y. Effects of ratio of radial partial air volume to pressure air volume on air curtain dust control at fully mechanized working face. *J. China Univ. Min. Technol.* **2017**, *46*, 1014−1023.

(3) Xu, G.; Chen, Y. P.; Eksteen, J.; Xu, J. L. Surfactant-aided coal dust suppression: a review of evaluation methods and influencing factors. *Sci. Total Environ.* **2018**, *639*, 1060−1076.

(4) Zhou, Q.; Xu, G.; Chen, Y. P.; Qin, B. T.; Zhao, Z. D.; Guo, C. W. The development of an optimized evaluation system for improving coal dust suppression efficiency using aqueous solution sprays. *Colloids Surf. A Physicochem. Eng. Asp.* **2020**, *602*, 125104.

(5) Li, J. Y.; Li, K. Q. Influence factors of coal surface wettability. *J. China Coal Soc.* **2016**, *41*, 448−453.

(6) Erbil, H. Y. The debate on the dependence of apparent contact angles on drop contact area or three-phase contact line: A review. *Surf. Sci. Rep.* **2014**, *69*, 325−365.

(7) Wang, K.; Ding, C. N.; Jiang, S. G.; Zhengyan, W.; Shao, H.; Zhang, W. Q. Application of the addition of ionic liquids using a

complex wetting agent to enhance dust control efficiency during coal mining. *Process Saf. Environ. Prot.* **2019**, *122*, 13−22.
(8) Zhao, B.; Li, S. G.; Lin, H. F.; Cheng, Y. Y.; Kong, X. G.; Ding, Y. Experimental study on the influence of surfactants in compound solution on the wetting-agglomeration properties of bituminous coal dust. *Powder Technol.* **2022**, *395*, 766−775.
(9) Liao, X. X.; Wang, L.; Zhu, J. T.; Chu, P.; Liu, Q. Q.; Yang, T. Experimental Study on the Wettability of Tectonic Soft Coal in Huaibei Mining Area, China. *Energy Fuel.* **2021**, *35*, 6585−6599.
(10) Xi, X.; Jiang, S. G.; Zhang, W. Q.; Wang, K.; Shao, H.; Wu, Z. Y. An experimental study on the effect of ionic liquids on the structure and wetting characteristics of coal. *Fuel* **2019**, *244*, 176−183.
(11) Feyyisa, J. L.; Daniels, J. L.; Pando, M. A. Contact angle measurements for use in specifying organosilane-modified coal combustion fly ash. *J. Mater. Civ. Eng.* **2017**, *29*, 04017096.
(12) Li, C.; Zhang, J.; Han, J.; Yao, B. H. A numerical solution to the effects of surface roughness on water−coal contact angle. *Sci. Rep.* **2021**, *11*, 459−512.
(13) Gui, Z.; Liu, R. H.; Wang, P. F.; Gou, S. X.; Shu, W.; Tan, X. H. Experimental study on surfactant effect on coal dust wettability. *J. Heilongjiang Univ. Sci. Technol.* **2016**, *26*, 513−517.
(14) Copeland, C. R.; Eisele, T. C.; Kawatra, S. K. Suppression of airborne particulates in iron ore processing facilities. *Int. J. Miner. Process.* **2009**, *93*, 232−238.
(15) Wang, X. N.; Yuan, S. J.; Li, X.; Jiang, B. Y. Synergistic effect of surfactant compounding on improving dust suppression in a coal mine in Erdos, China. *Powder Technol.* **2019**, *344*, 561−569.
(16) Jou, W. J.; Cao, Y. J.; Liu, J. T. Surface thermodynamic characterization of fine coal by Washburn dynamic method. *J. China Coal Soc.* **2013**, *38*, 1271−1276.
(17) Michel, J. C.; Riviere, L. M.; Bellon-Fontaine, M. N. Measurement of the wettability of organic materials in relation to water content by the capillary rise method. *Eur. J. Soil Sci.* **2001**, *52*, 459−467.
(18) Zhao, G. J.; Bi, S. S.; Wu, J. T.; Li, X. A new surface tension measurement system based on capillary rise method. *J. Eng. Thermophys.* **2011**, *32*, 546−548.
(19) Wu, C.; Peng, X. L.; Wu, G. M. Wetting agent investigation for controlling dust of lead-zinc ores. *Trans. Nonferrous Metals Soc. China* **2007**, *17*, 159−167.
(20) Jin, H.; Nie, W.; Zhang, H. H.; Liu, Y. H.; Bao, Q.; Wang, H. K.; Huang, D. M. Preparation and characterization of a novel environmentally friendly coal dust suppressant. *J. Appl. Polym. Sci.* **2019**, *136*, 47354.
(21) Yan, J. Y.; Nie, W.; Zhang, H. H.; Xiu, Z. H.; Bao, Q.; Wang, H. Q.; Jin, H.; Zhou, W. J. Synthesis and performance measurement of a modified polymer dust suppressant. *Adv. Powder Technol.* **2020**, *31*, 792−803.
(22) Wang, H. K.; Nie, W.; Zhang, H. H.; Jin, H.; Bao, Q.; Yan, J. Y.; Liu, Q. A synthesis of a dust suppressant using the cellulose extracted from maize straw. *Starch-Stärke* **2020**, *72*, 1900187.
(23) Zhang, H. H.; Nie, W.; Liu, Y. H.; Wang, H. K.; Jin, H.; Bao, Q. Synthesis and performance measurement of environment-friendly solidified dust suppressant for open pit coalmine. *J. Appl. Polym. Sci.* **2018**, *135*, 46505.
(24) Wang, H.; Wei, X. B.; Du, Y. H.; Wang, D. M. Effect of water-soluble polymers on the performance of dust-suppression foams: wettability, surface viscosity and stability. *Colloids Surf. A Physicochem. Eng. Asp.* **2019**, *568*, 92−98.
(25) Bao, Q.; Nie, W.; Liu, C. Q.; Zhang, H. H.; Wang, H. K.; Jin, H.; Yan, J. Y.; Liu, Q. The preparation of a novel hydrogel based on crosslinked polymers for suppressing coal dusts. *J. Clean. Prod.* **2020**, *249*, 119343.
(26) Zhang, H. H.; Nie, W.; Wang, H. K.; Bao, Q.; Jin, H.; Liu, Y. H. Preparation and experimental dust suppression performance characterization of a novel guar gum-modification-based environmentally-friendly degradable dust suppressant. *Powder Technol.* **2018**, *339*, 314−325.
(27) Jaiswal, A. K.; Khandekar, S. Drop-on-Drop Impact Dynamics on a Superhydrophobic Surface. *Langmuir* **2021**, *37*, 12629−12642.
(28) Josserand, C.; Thoroddsen, S. T. Drop impact on a solid surface. *Annu. Rev. Fluid. Mech.* **2016**, *48*, 365−391.
(29) Mundo, C. H. R.; Sommerfeld, M.; Tropea, C. Droplet-wall collisions: experimental studies of the deformation and breakup process. *Int. J. Multiphas. Flow* **1995**, *21*, 151−173.
(30) Yarin, A. L. Drop impact dynamics: splashing, spreading, receding, bouncing. *Annu. Rev. Fluid. Mech.* **2006**, *38*, 159−192.
(31) Han, Y.; Yang, Z. M.; He, L. M.; Luo, X. M.; Zhou, R. F.; Shi, K. Y.; Su, J. P. The influences of special wetting surfaces on the dynamic behaviors of underwater oil droplet. *Colloids Surf. A Physicochem. Eng. Asp.* **2018**, *543*, 15−27.
(32) Lunkad, S. F.; Buwa, V. V.; Nigam, K. D. P. Numerical simulations of drop impact and spreading on horizontal and inclined surfaces. *Chem. Eng. Sci.* **2007**, *62*, 7214−7224.
(33) Liu, X. H.; Wang, K. M.; Fang, Y. Q.; Goldstein, R. J.; Shen, S. Q. Study of the effect of surface wettability on droplet impact on spherical surfaces. *Int. J. Low Carbon Technol.* **2020**, *15*, 414−420.
(34) Liu, X.; Min, J. C.; Zhang, X. Dynamic behavior and maximum spreading of droplets impacting concave spheres. *Phys. Fluids* **2020**, *32*, 092109.
(35) Banks, D.; Ajawara, C.; Sanchez, R.; Surti, H.; Aguilar, G. Effects of liquid and surface characteristics on oscillation behavior of droplets upon impact. *Atomization Sprays* **2014**, *24*, 895−913.
(36) Nefzaoui, E.; Skurtys, O. Impact of a liquid drop on a granular medium: Inertia, viscosity and surface tension effects on the drop deformation. *Exp. Therm. Fluid Sci.* **2012**, *41*, 43−50.
(37) You, X. F.; He, M.; Cao, X. Q.; Wang, P.; Wang, J. X.; Li, L. Molecular dynamics simulations of removal of nonylphenol pollutants by graphene oxide: Experimental study and modelling. *Appl. Surf. Sci.* **2019**, *475*, 621−626.
(38) Xu, C. H.; Wang, D. M.; Wang, H. T.; Ma, L. Y.; Zhu, X. L.; Zhu, Y. F.; Zhang, Y.; Liu, F. M. Experimental investigation of coal dust wetting ability of anionic surfactants with different structures. *Process Saf. Environ. Prot.* **2019**, *121*, 69−76.
(39) Alghunaim, A.; Kirdponpattara, S.; Newby, B. m. Z. Techniques for determining contact angle and wettability of powders. *Powder Technol.* **2016**, *287*, 201−215.
(40) Qin, M. X.; Tang, C. L.; Tong, S. Q.; Zhang, P.; Huang, Z. H. On the role of liquid viscosity in affecting droplet spreading on a smooth solid surface. *Int. J. Multiphase Flow* **2019**, *117*, 53−63.
(41) Clanet, C.; Béguin, C.; Richard, D.; Quéré, D. Maximal deformation of an impacting drop. *J. Fluid Mech.* **2004**, *517*, 199−208.
(42) Bayer, I. S.; Megaridis, C. M. Contact angle dynamics in droplets impacting on flat surfaces with different wetting characteristics. *J. Fluid Mech.* **2006**, *558*, 415−449.
(43) Roisman, I. V. Inertia dominated drop collisions. II. An analytical solution of the Navier−Stokes equations for a spreading viscous film. *Phys. Fluids* **2009**, *21*, 052104.

https://doi.org/10.1021/acsomega.2c07783
ACS Omega 2023, 8, 18414−18424